



HAL
open science

Macroscopic inelastic behaviors simulated by a stochastic multi-scale numerical model for heterogeneous materials

Pierre Jehel

► **To cite this version:**

Pierre Jehel. Macroscopic inelastic behaviors simulated by a stochastic multi-scale numerical model for heterogeneous materials. 13th World Congress on Computational Mechanics (WCCM XIII), Jul 2018, New York, United States. hal-01846149

HAL Id: hal-01846149

<https://hal.science/hal-01846149>

Submitted on 24 Jul 2018

HAL is a multi-disciplinary open access archive for the deposit and dissemination of scientific research documents, whether they are published or not. The documents may come from teaching and research institutions in France or abroad, or from public or private research centers.

L'archive ouverte pluridisciplinaire **HAL**, est destinée au dépôt et à la diffusion de documents scientifiques de niveau recherche, publiés ou non, émanant des établissements d'enseignement et de recherche français ou étrangers, des laboratoires publics ou privés.

MACROSCOPIC INELASTIC BEHAVIORS SIMULATED BY A STOCHASTIC MULTI-SCALE NUMERICAL MODEL FOR HETEROGENEOUS MATERIALS

PIERRE JEHEL

Laboratory MSSMat-UMR 8579 (CentraleSupélec/CNRS)
Université Paris-Saclay, CentraleSupélec, 3 rue Joliot-Curie, 91190 Gif-sur-Yvette, France
E-mail: pierre.jehel[at]centralesupelec.fr

Key words: Random heterogenous material; Inelastic cyclic behavior; Uncertainty quantification; Global sensitivity analysis; Variance decomposition.

Abstract. *The uncertainty and the sensitivity of the response of a nonlinear stochastic multi-scale numerical model for randomly heterogenous material is investigated. 9 input parameters and 10 descriptors of the time-dependent output response are considered. The material model has been presented elsewhere and is introduced as a 'black box function' in the present paper, parameterized so that the model is deterministic and that variability in the outputs only comes from the variability introduced in the inputs. The objective is twofolds: (i) surveying the variety of macroscopic behaviors the material model considered is capable of representing, and (ii) assessing the relative importance of the model inputs in the model outputs to, for instance, define efficient parameters identification protocols. A preliminary analysis of the linear dependency between the output descriptors is presented and a reduced set of 6 descriptors is eventually selected. Then, the influence of the model input parameters on each of these model response descriptors is investigated using a global sensitivity analysis technique based on the functional decomposition of their respective total variance.*

1 INTRODUCTION

The mechanical behavior of a wide range of natural or manufactured materials is characterized by macroscopic engineering parameters that depend on phenomena at heterogeneous smaller scales (concrete, nano-engineered materials [12]). On the one hand, experimental devices and techniques allow characterizing the spatial distribution of material properties at micro-scales as for instance the combination of atomic force microscope imaging and quantitative nanomechanical property mapping techniques employed in [14] for a study of Young's modulus distribution in the so-called interfacial transition zone in concrete material. On the other hand, computational material models allow carrying out numerical experiments that have the potential of investigating the material behavior in a range of configurations that can be difficult to reach with sole experimental investigation. There is therefore a need for developing such numerical material models that can simulate engineering properties at macro-scale from relevant

information coming from lower scales. This has been a topic of continuing research in the field of computational mechanics for decades.

The development of the inelastic stochastic multi-scale numerical model investigated in the present work (see [5] and [6]) was initially motivated by the need for a concrete model that is capable of representing the contribution of material damping to the overall structural damping in the seismic analysis of civil engineering assets. In earthquake engineering, structural damping is indeed commonly introduced in numerical simulations using ad hoc damping models such as the pervasive so-called Rayleigh damping model. Unfortunately, as nonlinear structural analysis is performed, resorting to such ad hoc approach potentially results in large uncertainties when assessing structural seismic performance.

This concrete model [5, 6] is based on a meso-scale where the heterogeneous structure is represented by random vector fields. Local behavior at meso-scale is nonlinear and can be seen as the homogenized response of other mechanisms at lower scales when explicit construction of smaller scales is not possible. The model is constructed with a set of parameters that describes the structure of the random vector fields (correlation coefficients, correlation lengths and functions); a set of parameters that characterizes the mean, variance and distribution of physical parameters at meso-scale (initial stiffness, yield stress and stiffness degradation ratio); and a set of parameters for spatial discretization of the material domain (finite element method) and of the random fields (spectral representation method [11]). A representative volume element (RVE) can be retrieved with the ability to represent salient features of the concrete uniaxial cyclic compressive response that are not explicitly represented at meso-scale, like for instance the hysteresis loops experimentally observed in unloading-reloading cycles.

The objective of this paper is twofolds: (i) surveying the variety of macroscopic behaviors this numerical inelastic stochastic multi-scale material model is capable of representing, and (ii) assessing the relative importance of the model inputs in the model outputs to, for instance, define efficient parameters identification protocols. Next section is focussed on introducing the model input parameters. Then, a probabilistic framework is set in section 3 for uncertainty and global sensitivity analysis. In section 4, the results of an application are presented and, finally, a list of conclusions closes the paper.

2 THE MATERIAL MODEL AND ITS INPUT PARAMETERS

The material model used in this paper has been developed to represent the restoring force $f(t)$ of a 1D nonlinear material in a given cyclic quasi-static loading displacement time history $u(t)$ where t is the pseudo-time (Fig. 1). This material model is referred to as \mathcal{M} , it takes t along with a set of parameters \mathbf{x} as inputs, and yields the restoring force history $f(t)$ as output.

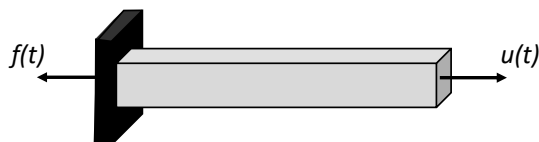


Figure 1: The experiment: bar with quasi-static displacement $u(t)$ imposed at one end, with other end fixed where reaction $f(t)$ develops; it is assumed that the experiment is such that the strain field is homogeneous in the bar.

The material model \mathcal{M} that is used in this work has been presented in [5, 6]. Therefore, we only introduce here its main characteristics along with the list of input parameters that will be used for uncertainty and sensitivity analyses hereafter. Also, for the sake of illustrating, we

consider that the modeled material is concrete; but any other random heterogeneous material described by 3 scales as introduced in Tab. 1 and Fig. 2 could fit this setting.

Scale	Observations	Modeling assumptions
Micro	Physical and chemical mechanisms occur	Internal variables are considered in the framework of continuum thermodynamics [1, 8] to convey information from this scale to the meso-scale (see Fig. 3).
Meso	Aggregates and the cement paste are observable and build an heterogeneous material structure	The heterogeneity at this scale is represented using random fields rather than an explicit representation of the structure.
Macro	Homogeneous quantities are retrieved for engineering purposes	Classical homogenization technique in the framework of the Finite Element Method is used [9, 10].

Table 1: The 3 scales introduced in the model \mathcal{M} . Concrete material is considered here as an illustrating example.

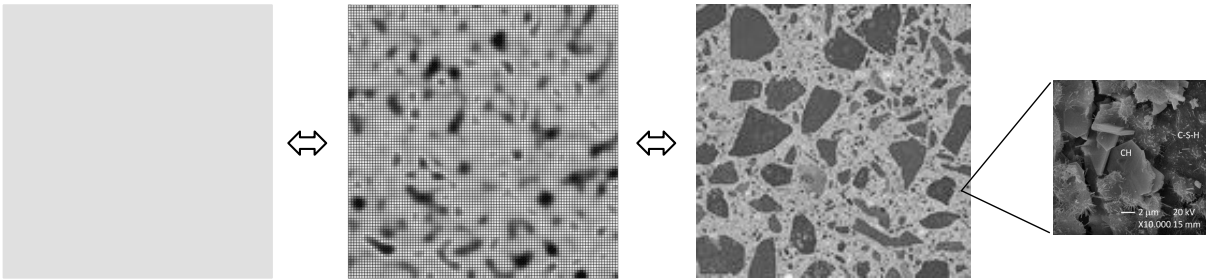


Figure 2: From left to right: [a] equivalent homogeneous concrete (macro-scale), [b] representation of the heterogeneous concrete at meso-scale ($5 \text{ cm} \times 5 \text{ cm}$ -square), [c] actual heterogeneous concrete ($5 \text{ cm} \times 5 \text{ cm}$ -square), and [d] zoom on the underlying microstructure in the cement paste ($20 \mu\text{m} \times 20 \mu\text{m}$ -square observed through Scanning Electron Microscope, courtesy A.P.M. Trigo [13]).

The model uses stochastic fields to represent spatial variations – that is random heterogeneity – in the material properties at meso-scale. The actual meso-scale shown in Fig. 2[c] is replaced by random vector fields as shown in Fig. 2[b]. In the particular case of a 1D material behavior, which this work is limited to, three parameters are represented as spatially variable as illustrated in Fig. 3: the initial stiffness $C(\mathbf{p}, \omega)$ (or Young’s modulus at meso-scale), the yield stress $\sigma_y(\mathbf{p}, \omega)$, and the stiffness degradation ratio $r(\mathbf{p}, \omega) \in [0, 1]$, where \mathbf{p} is a position in the material and ω recalls the randomness in the quantity. The three quantities are correlated and the same correlation coefficient ρ is considered for any pair of parameters. The parameters \mathbf{x} of model \mathcal{M} are listed in Tab. 2.

The model \mathcal{M} can be stochastic: same input parameters \mathbf{x} and imposed displacement history $u(t)$ can yield different outputs. Nevertheless, it has been shown in [5, 6] that the model can also be deterministic: same input parameters \mathbf{x} and loading history $u(t)$ would yield same output. In other words, it is possible to parameter the model in such a way that a material Representative Volume Element (RVE) is simulated. This can be achieved using particular set of spatial parameters ($N = 16$, $M = 32$, $M_f = 96$, $L_0/\ell = 0.1$, $\epsilon_R = 0.01$ using the same notations as in [5]). This parameterization is used in this paper so that uncertainty observed in the output parameters \mathbf{y} would only come from uncertain input parameters \mathbf{x} .

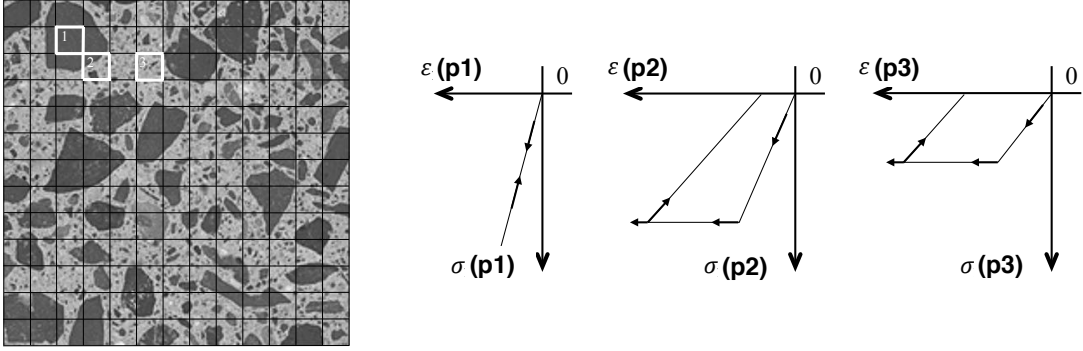


Figure 3: Behavior law at meso-scale depends on the position \mathbf{p} in the heterogeneous material. Initial stiffness, yield stress, and stiffness degradation ratio at any point \mathbf{p} are modeled as random variables.

\mathbf{x}	Description
$x_1 = law_C$	Initial stiffness C distribution (log-normal or uniform)
$x_2 = a_C$	Mean of law_C
$x_3 = b_C$	Variance of law_C
$x_4 = law_{\sigma_y}$	Yield stress σ_y distribution (log-normal or uniform)
$x_5 = a_{\sigma_y}$	Mean of law_{σ_y}
$x_6 = b_{\sigma_y}$	Variance of law_{σ_y}
$x_7 = a_r$	Mean of the stiffness degradation ratio uniform distribution law_r
$x_8 = b_r$	Variance of law_r
$x_9 = \rho$	Correlation coefficient between $(C$ and $\sigma_y)$, $(C$ and $r)$, or $(\sigma_y$ and $r)$

Table 2: List of the $N^x = 9$ model input parameters $x_j, j = 1 \dots N^x$ considered in this work.

3 UNCERTAINTY AND SENSITIVITY ANALYSES OF THE MODEL OUTPUT

Let introduce the probability space (Θ, \mathcal{S}, P) with sample space Θ , collection of events \mathcal{S} , and probability measure P . To introduce a certain degree of belief in the set \mathbf{x} of the model input parameters, we consider them as random variables $\mathbf{X} : \theta \in \Theta \mapsto \mathbf{X}(\theta)$. Consequently, the model output $f(t)$ also is a random variable $F(t) : \theta \mapsto F(t, \theta)$ for all $t \in [0, T]$ and we have the deterministic model \mathcal{M} that is the mapping

$$\mathcal{M} : (\theta, t) \mapsto F(t) = \mathcal{M}(\mathbf{X}, t) \quad (1)$$

3.1 Uncertainty analysis

The uncertainty in the model output can be analyzed computing quantities such as the mean, variance, and cumulated density function for all $t \in [0, T]$:

$$E[F(t)] = \int_{\Theta} \mathcal{M}(\mathbf{X}(\theta), t) dP(\theta) \quad (2)$$

$$V[F(t)] = \int_{\Theta} (E[F(t)] - \mathcal{M}(\mathbf{X}(\theta), t))^2 dP(\theta) \quad (3)$$

$$\Pr[F(t) \leq f(t)] = \int_{\Theta} \delta_{f(t)}[\mathcal{M}(\mathbf{X}(\theta), t)] dP(\theta) \quad \text{with} \quad \delta_{f(t)}[\cdot] = \begin{cases} 1 & \text{if } \cdot \leq f(t) \\ 0 & \text{if } \cdot > f(t) \end{cases} \quad (4)$$

This requires computing integrals over the sample space Θ . To this purpose, Monte Carlo simulations are performed from a Latin hypercube sample (LHS) of size N^s . LHS is adopted here for its efficiency compared to random sampling [3, 7] with the N^x input random variables in \mathbf{X} assumed as mutually independent.

3.2 Sensitivity analysis

For the analysis of the sensitivity of the model output to the inputs, the approach adopted in this work is based on a functional decomposition of the variance (see e.g. [4]), $\forall t \in [0, T]$, as:

$$V[F(t)] = \sum_{j=1}^{N^x} D_j[F(t)] + \sum_{1 \leq j < k \leq N^x} D_{jk}[F(t)] + \dots + D_{12\dots N^x}[F(t)] \quad (5)$$

where $D_j[F(t)] = V[E[F(t)|X_j]]$, $D_{jk}[F(t)] = V[E[F(t)|X_j, X_k]] - D_j[F(t)] - D_k[F(t)]$ and so on. Then, the following first-order and total indices are computed from $(N^x + 2) \times N^s$ computations of the model response as:

$$s_j = \frac{D_j[F(t)]}{V[F(t)]} \quad (6)$$

$$s_{jT} = s_j + \frac{\sum_{k=1, k \neq j}^{N^x} D_{jk} + \sum_{1 \leq k \neq j < l \neq j}^{N^x} D_{jkl} + \dots + D_{12\dots N^x}}{V[F(t)]} \quad (7)$$

where s_j , respectively s_{jT} , is the portion of $V[F(t)]$ due to input x_j alone, respectively to x_j and all the interactions of x_j with the other input variables.

4 APPLICATION

4.1 Uncertainty in the model input parameters

The distributions selected for the uncertain input parameters are introduced in Tab. 3.

$\mathbf{X}(\theta)$	Distribution: <i>law(mean, variance)</i>	
$X_1 = LAW_C$	$\mathcal{B}_{0.5}$: either $\mathcal{U}(a_C, b_C)$ or $\mathcal{L}(a_C, b_C)$	with probability 0.5 each
$X_2 = A_C$ [MPa]	$\mathcal{U}(\tilde{a}_C = 30e3, 0.04 \tilde{a}_C^2)$	such that $C \geq 0$
$X_3 = B_C$ [MPa ²]	$\mathcal{U}(\tilde{b}_C = 15e3, 0.04 \tilde{b}_C^2)$	such that $C \geq 0$
$X_4 = LAW_{\sigma_y}$	$\mathcal{B}_{0.5}$: either $\mathcal{U}(a_{\sigma_y}, b_{\sigma_y})$ or $\mathcal{L}(a_{\sigma_y}, b_{\sigma_y})$	with probability 0.5 each
$X_5 = A_{\sigma_y}$ [MPa]	$\mathcal{U}(\tilde{a}_{\sigma_y} = 35, 0.04 \tilde{a}_{\sigma_y}^2)$	such that $\sigma_y \geq 0$
$X_6 = B_{\sigma_y}$ [MPa ²]	$\mathcal{U}(\tilde{b}_{\sigma_y} = 20, 0.04 \tilde{b}_{\sigma_y}^2)$	such that $\sigma_y \geq 0$
$X_7 = A_r$	$\mathcal{U}(\tilde{a}_r = 0.5, 0.04 \tilde{a}_r^2)$	such that $r \in [0, 1]$
$X_8 = B_r$	$\mathcal{U}(\tilde{b}_r = 0.02, 0.04 \tilde{b}_r^2)$	such that $r \in [0, 1]$
$X_9 = Rho$	$\mathcal{U}(0.5, 1/12)$	(support is $[0, 1]$)

Table 3: Random variables and there distributions characterized by their mean and variance. \mathcal{B} , \mathcal{U} , and \mathcal{L} are Bernoulli, uniform, and log-normal distributions. How to find the support of a uniform distribution from its mean and variance is shown in the Annex. Quantities with superimposed tilde $\tilde{\cdot}$ are some nominal mean values; a coefficient of variation of 20% is considered to calculate the variance associated to these nominal mean values.

4.2 Model response descriptors

We start by simulating the material response in one symmetric loading cycle with macroscopic strain amplitude $E = 3.5e^{-3}$. $N^s = 500$ simulations are run and model responses are plot in Fig. 4. From the observation of this figure we choose a series of N^y model response descriptors as introduced in Fig. 5, gathered in vector y . Then, we seek possible linear dependencies – other types of dependencies could of course be sought too – and build Fig. 6. From Fig. 6, it is observed that model response after point D is strongly correlated to model response between points O and D. Accordingly, only the following $N^y = 6$ model response descriptors will be considered thereafter: $y_1 = C_O$, $y_2 = C_B$, $y_3 = \Sigma_A$, $y_4 = \Sigma_B$, $y_5 = \Sigma_D$, and $y_6 = E_C$.

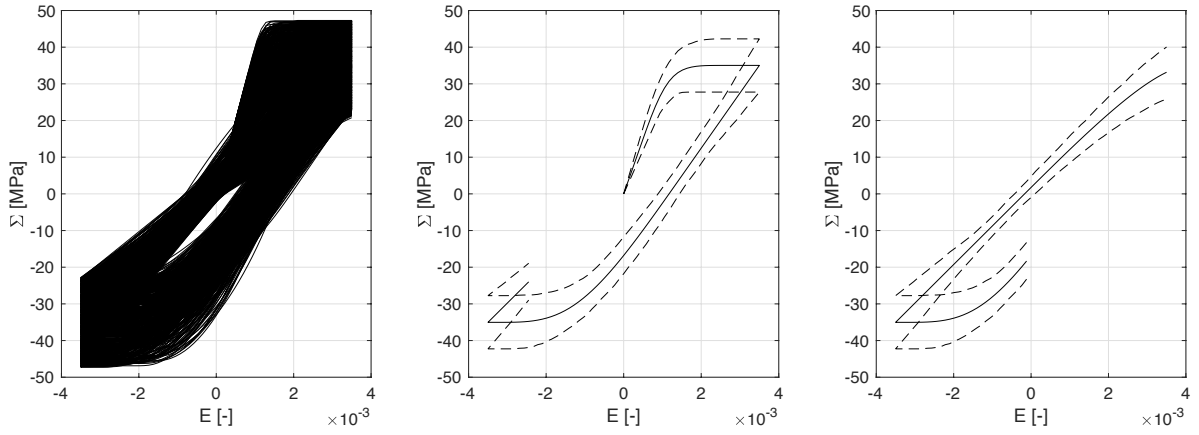


Figure 4: [left] $N^s = 500$ model response curves. [middle] and [left] Sample mean along with the 10% and 90% percentiles (dashed line); response curves are split into two parts for better readability.

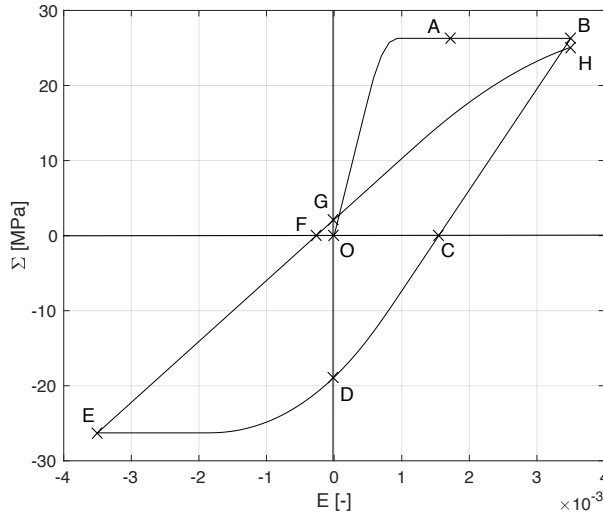


Figure 5: Model response descriptors: initial tangent modulus C_O and unloading tangent modulus at point B C_B ; stresses Σ_A ($E = 1.75e^{-3}$), Σ_B , Σ_D , Σ_E , Σ_G , and Σ_H ; strains E_C and E_F .

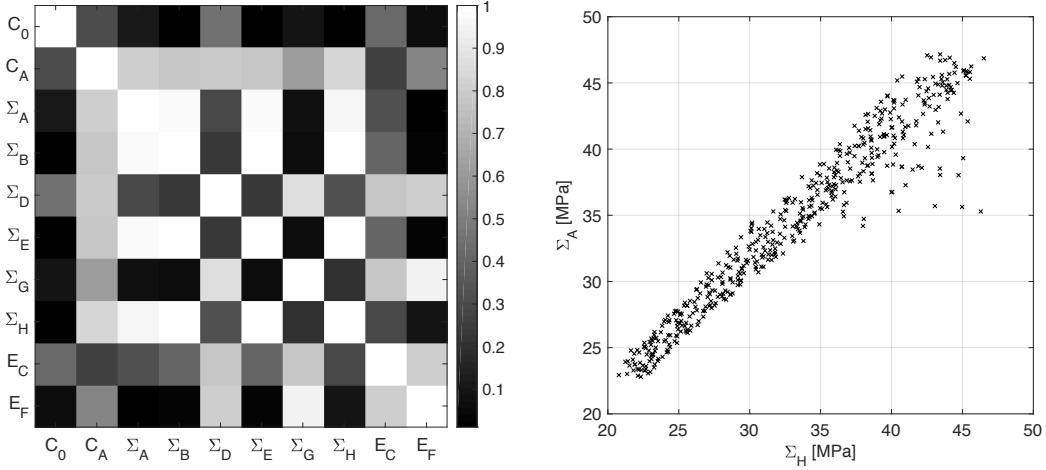


Figure 6: [left] Absolute value of the sample Pearson correlation coefficients between model response descriptors y_k , $k = 1 \dots N^y$; [right] scatterplot of Σ_A versus Σ_H showing strong linear correlation.

4.3 Uncertainty and sensitivity estimators

To estimate global sensitivity of the model outputs \mathbf{y} to the inputs \mathbf{x} , the method detailed in [2] (Sect. 6.13) has been implemented. Accordingly:

1. A first LHS $[x_{ij}]$, $i \in [0, N^s]$ and $j \in [0, N^x]$, is generated and the model response $\mathbf{y}_i(t) = \mathcal{M}(\mathbf{x}_i, t)$ is computed for each set of input parameters $\mathbf{x}_i = [x_{i1} \dots x_{iN^x}]$. From these quantities, estimators of the mean and variance in Eqs. (2) and (3) are computed $\forall k \in [1 \dots N^y]$ as:

$$\hat{E}[Y_k] = \frac{1}{N^s} \sum_{i=1}^{N^s} y_{k,i}(t) \quad ; \quad \hat{V}[Y_k] = (\hat{\sigma}[Y_k])^2 = \frac{1}{N^s} \sum_{i=1}^{N^s} (\hat{E}[Y_k] - y_{k,i}(t))^2 \quad (8)$$

2. Another sample $[\bar{x}_{I,j}] = [p(\mathbf{x}_1) \dots p(\mathbf{x}_{N^s})]$, $I \in [0, N^s]$, is built, where $p(\mathbf{x}_j)$ is a random permutation without replacement of the N^s elements of the j -th column of $[x_{ij}]$. The model response $\bar{\mathbf{y}}_I(t) = \mathcal{M}(\bar{\mathbf{x}}_I, t)$ is computed for each $\bar{\mathbf{x}}_I = [\bar{x}_{I1} \dots \bar{x}_{IN^x}]$. Then, N^x samples of N^s model responses are obtained by reordering the computed $\bar{\mathbf{y}}_I(t)$'s as follows: $\bar{\mathbf{y}}_i^{(j)}(t) = \mathcal{M}([\bar{x}_{I1} \dots \bar{x}_{Ij} = x_{ij} \dots \bar{x}_{IN^x}], t)$, $j \in [0, N^x]$.
3. A last LHS $[\check{x}_{ij}]$, $i \in [0, N^s]$ and $j \in [0, N^x]$, is generated and N^x samples of N^s model responses are computed as $\bar{\mathbf{y}}_i^{(j)} = \mathcal{M}(\bar{\mathbf{x}}_i^{(j)}, t)$, $\bar{\mathbf{x}}_i^{(j)} = [\bar{x}_{i1}^{(j)} \dots \bar{x}_{iN^x}^{(j)}]$, with $\bar{x}_{iJ}^{(j)} = x_{iJ}$ for $J \in [0, N^x]$ except for $J = j$ where $\bar{x}_{iJ}^{(j)} = \check{x}_{ij}$.

Estimators for the sensitivity indices are then computed, $\forall k \in [1 \dots N^y]$, as:

$$\hat{s}_{k,j} = \frac{1}{\hat{V}[Y_k]} \left(\frac{1}{N^s} \sum_{i=1}^{N^s} y_{k,i}(t) \times \bar{y}_{k,i}^{(j)}(t) - \hat{E}[Y_k]^2 \right) \quad (9)$$

$$\hat{s}_{k,jT} = \frac{1}{N^s \times \hat{V}[Y_k]} \sum_{i=1}^{N^s} y_{k,i} \left(y_{k,i} - \bar{y}_{k,i}^{(j)} \right) \quad (10)$$

Altogether, the model has to be run $(2 + N^x) \times N^s$ times. In the present work, $N^x = 9$, $N^s = 300, 400$, or $1,000$, and computing one model response takes less than 2 seconds. The calculated estimations are shown in Tab. 4.

	N^s	$y_1 = C_0$	$y_2 = C_B$	$y_3 = \Sigma_A$	$y_4 = \Sigma_B$	$y_5 = \Sigma_D$	$y_6 = E_C$
$\hat{E}[Y_k]$	300	29,998 MPa	15,034 MPa	34.470 MPa	35.034 MPa	-16.801 MPa	1.156e-3
	600	29,997 MPa	15,040 MPa	34.441 MPa	35.035 MPa	-16.776 MPa	1.155e-3
	1,000	29,997 MPa	15,008 MPa	34.344 MPa	35.030 MPa	-16.700 MPa	1.152e-3
$\hat{\sigma}[Y_k]$	300	6,001 MPa	2,822 MPa	6.565 MPa	7.007 MPa	5.509 MPa	3.06e-4
	600	6,000 MPa	2,848 MPa	6.507 MPa	7.000 MPa	5.561 MPa	3.09e-4
	1,000	6,000 MPa	2,835 MPa	6.413 MPa	7.006 MPa	5.494 MPa	3.04e-4
$\hat{s}_1 (x_1 = law_C)$	300	0.012	0.058	0.112	0.056	-0.012	0.058
	600	-0.074	-0.021	-0.003	-0.029	-0.050	-0.068
	1,000	0.003	-0.006	0.119	-0.011	0.046	0.075
$\hat{s}_2 (x_2 = a_C)$	300	1.000	0.070	-0.018	-0.104	0.256	0.269
	600	1.000	0.127	0.068	0.016	0.268	0.225
	1,000	1.000	0.159	0.137	-0.018	0.294	0.204
$\hat{s}_3 (x_3 = b_C)$	300	0.077	0.087	-0.004	-0.081	0.083	0.062
	600	-0.015	0.013	0.022	-0.021	-0.003	-0.039
	1,000	0.008	0.029	0.157	0.017	-0.028	-0.034
$\hat{s}_4 (x_4 = law_{\sigma_y})$	300	-0.024	0.167	0.135	0.048	0.112	0.144
	600	-0.056	0.028	-0.004	-0.038	0.063	0.025
	1,000	-0.011	0.056	0.149	0.017	0.076	0.072
$\hat{s}_5 (x_5 = a_{\sigma_y})$	300	-0.042	0.626	1.032	1.002	0.023	0.218
	600	-0.034	0.573	0.994	1.000	0.014	0.131
	1,000	-0.014	0.614	1.103	1.003	0.046	0.187
$\hat{s}_6 (x_6 = b_{\sigma_y})$	300	-0.078	0.030	0.035	-0.014	-0.034	0.022
	600	0.003	0.042	0.054	-0.016	-0.017	-0.114
	1,000	0.004	0.017	0.106	-0.018	0.016	0.012
$\hat{s}_7 (x_7 = a_r)$	300	-0.070	0.331	0.097	0.049	0.679	0.709
	600	0.011	0.300	0.040	0.030	0.644	0.595
	1,000	0.029	0.335	0.130	0.002	0.697	0.618
$\hat{s}_8 (x_8 = b_r)$	300	-0.066	-0.004	0.074	0.016	-0.034	0.073
	600	0.026	0.000	-0.012	-0.049	-0.003	-0.075
	1,000	0.011	0.088	0.173	0.042	0.076	0.058
$\hat{s}_9 (x_9 = \rho)$	300	-0.021	0.066	0.102	0.019	-0.053	-0.041
	600	-0.007	0.006	0.063	0.015	-0.007	0.008
	1,000	-0.074	0.010	0.115	-0.001	0.011	0.034
$\hat{s}_{1T} (x_1 = law_C)$	300	0.000	0.000	-0.001	0.000	0.002	-0.002
	600	0.000	-0.002	0.002	0.002	-0.003	0.004
	1,000	0.000	0.000	0.000	-0.000	0.001	-0.001
$\hat{s}_{2T} (x_2 = a_C)$	300	1.020	0.038	0.017	-0.002	0.212	0.179
	600	0.914	0.230	0.046	0.002	0.374	0.297
	1,000	0.945	0.067	-0.083	-0.001	0.246	0.202
$\hat{s}_{3T} (x_3 = b_C)$	300	0.000	0.001	0.000	0.000	0.004	-0.002
	600	0.000	0.000	0.001	0.001	-0.001	0.000
	1,000	0.000	-0.001	0.000	0.000	-0.003	-0.001
$\hat{s}_{4T} (x_4 = law_{\sigma_y})$	300	0.000	0.000	-0.005	-0.002	0.019	-0.001
	600	0.000	0.002	-0.004	-0.001	0.008	-0.004
	1,000	0.000	0.000	-0.003	-0.002	0.001	-0.001
$\hat{s}_{5T} (x_5 = a_{\sigma_y})$	300	0.000	0.581	0.894	0.939	0.111	0.180
	600	0.000	0.547	0.920	1.005	0.049	0.223
	1,000	0.000	0.565	0.893	1.023	0.078	0.171
$\hat{s}_{6T} (x_6 = b_{\sigma_y})$	300	0.000	-0.002	0.007	-0.004	0.006	0.001
	600	0.000	-0.003	0.004	0.001	-0.003	-0.004
	1,000	0.000	-0.001	0.000	-0.000	-0.002	-0.001
$\hat{s}_{7T} (x_7 = a_r)$	300	0.000	0.174	-0.003	-0.003	0.572	0.554
	600	0.000	0.316	0.000	0.000	0.619	0.566
	1,000	0.000	0.343	-0.004	-0.003	0.721	0.607
$\hat{s}_{8T} (x_8 = b_r)$	300	0.000	-0.008	-0.001	0.000	0.002	-0.008
	600	0.000	-0.006	0.002	0.002	0.001	-0.007
	1,000	0.000	-0.004	-0.001	-0.000	-0.004	-0.003
$\hat{s}_{9T} (x_9 = \rho)$	300	0.000	0.000	0.000	0.000	-0.001	0.002
	600	0.000	0.007	0.003	0.005	0.012	0.007
	1,000	0.000	0.009	-0.004	-0.004	-0.005	0.021

Table 4: Estimates $\hat{E}[Y_k]$ and $\hat{\sigma}[Y_k]$ for expected value and standard deviation of the model response descriptors y_k with $k = 1 \dots N^y$; estimates \hat{s}_j for the contribution of each input x_j with $j = 1 \dots N^x$; estimates \hat{s}_{jT} for the contribution of each input x_j and all its interactions with the other inputs x_p with $p = 1 \dots N^x$ and $p \neq j$.

5 CONCLUSIONS

In the particular case of the experiment shown in Fig. 1, and from the above presented work, the following conclusions can be drawn about the inelastic stochastic multi-scale numerical model for random heterogeneous materials developed in [5] and [6]:

- Fig. 4: The model simulates macroscopic behaviors of analogous shapes for all the sets of input parameters considered.
- Tab. 4: Clear trends regarding the relative importance of the model input parameters on the outputs can be observed with a relatively small number of simulations.
- Tab. 4: 3 out of 9 input parameters are key to control the simulated macroscopic response, namely the means of the random fields at meso-scale: a_C , a_{σ_y} , and a_r .
- Tab. 4: Combined actions of two or more input parameters on the model outputs are very limited ($\hat{s}_{k,j} \approx \hat{s}_{k,jT}$, $\forall (j, k) \in [1, N^x] \times [1, N^y]$).
- Tab. 4: Initial stiffness C_O at macro-scale solely depends on the mean a_C of the initial stiffness marginal distribution at meso-scale (see Fig. 4). This is in accordance with the way the model is built: by definition $C_O = \langle C(\mathbf{p}, \omega) \rangle$ with $\langle C(\mathbf{p}, \omega) \rangle$ the spatial mean of the initial stiffness field over the material RVE, and, consequently to ergodicity properties of the random vector field at meso-scale $a_C = \langle C(\mathbf{p}, \omega) \rangle$; accordingly: $C_O = a_C$.

ACKNOWLEDGEMENT

Part of this work has been developed while visiting the Department of Civil Engineering and Engineering Mechanics at Columbia University in the City of New York.

REFERENCES

- [1] Germain P., Nguyen Q.S., Suquet P. Continuum thermodynamics. ASME Journal of Applied Mechanics (1983) 50:1010–1020.
- [2] Helton J.C., Johnson J.D., Sallaberry C.J., Storlie C.B. Survey of sampling-based methods for uncertainty and sensitivity analysis. Reliability Engineering & System Safety (2006) 91:1175–1209.
- [3] Helton J.C., Davis F.J. Latin hypercube sampling and the propagation of uncertainty in analyses of complex systems. Reliability Engineering & System Safety (2003) 81:23–69.
- [4] Iooss B., Lemaître P. *A review on global sensitivity analysis methods*. In: Meloni C. and Dellino G. (Eds.) Uncertainty management in Simulation-Optimization of Complex Systems: Algorithms and Applications, Springer, 2015.
- [5] Jehel P. A Stochastic Multi-scale Approach for Numerical Modeling of Complex Materials – Application to Uniaxial Cyclic Response of Concrete. In: Ibrahimbegovic A. (ed.), Computational Methods for Solids and Fluids. Springer, pp. 123–160 (2016).
- [6] Jehel P., Cottureau R. On damping created by heterogeneous yielding in the numerical analysis of nonlinear reinforced concrete frame elements. Computers and Structures (2015) 154:192–203.

- [7] Mc Kay M.D., Conover W.J., Beckman, R.J. A comparison of three methods for selecting values of input variables in the analysis of output from a computer code. *Technometrics* (1979) 21:239–245.
- [8] Maugin G. The thermodynamics of nonlinear irreversible behaviors: An introduction. World Scientific, Singapore (1999).
- [9] Miehe C., Koch A. Computational micro-to-macro transitions of discretized microstructures undergoing small strains. *Archive of Applied Mechanics* (2002) 72:300–317.
- [10] Nemat-Nasser S., Hori M. *Micromechanics: Overall properties of heterogenous materials*. Elsevier Science Publishers B.V., Amsterdam, The Netherlands (1993).
- [11] Popescu R., Deodatis G., Prevost J.H. Simulation of homogeneous nonGaussian stochastic vector fields. *Probabilistic Engineering Mechanics* (1998) 13(1):1–13.
- [12] Savvas D., Stefanou G., Papadopoulos V., Papadrakakis M. Effect of waviness and orientation of carbon nanotubes on random apparent material properties and RVE size of CNT reinforced composites. *Composite Structures* (2016) 152:870–882.
- [13] Trigo A.P.M., Liborio J.B.L. Doping technique in the interfacial transition zone between paste and lateritic aggregate for the production of structural concretes. *Materials Research* (2014) 17(1):16–22.
- [14] Zhu X., Gao Y., Dai Z., Corr D.J., Shah S.P. Effect of interfacial transition zone on the Young’s modulus of carbon nanofiber reinforced cement concrete. *Cement and Concrete Research* (2018) 107:49–63.

ANNEX - Support of a uniform distribution with know mean and variance

Let $\mathcal{U}(a, b)$ be a uniform distribution over the range $[x; y]$ ($x < y$) with mean a and variance $b^2 > 0$. In this annex, we show how to calculate x and y from a and b . By definition, the following nonlinear system has to be solved:

$$\begin{cases} x + y = 2a \\ (y - x)^2 = 12b^2 \end{cases} \quad (11)$$

Introducing $C^2 = 4a^2$ and $D^2 = 12b^2$, Eqs. (11) implies that:

$$\begin{cases} (x + y)^2 = C^2 \\ (x - y)^2 = D^2 \end{cases} \Rightarrow \begin{cases} x + y = \pm C \\ x - y = \pm D \end{cases} \quad (12)$$

Consequently, we have the following four possible couples of solutions:

$$\begin{aligned} (x_1, y_1) &= ((C + D)/2, (C - D)/2) \\ (x_2, y_2) &= ((C - D)/2, (C + D)/2) \\ (x_3, y_3) &= ((-C + D)/2, (-C - D)/2) \\ (x_4, y_4) &= ((-C - D)/2, (-C + D)/2) \end{aligned} \quad (13)$$

From Eqs. (13), the following table can be built:

i	$(x_i + y_i)/2$	$x_i - y_i$	$(C, D) = (2a, \sqrt{12}b)$	$(C, D) = (2a, -\sqrt{12}b)$	$(C, D) = (-2a, \sqrt{12}b)$	$(C, D) = (-2a, -\sqrt{12}b)$
1	$C/2$	D	<i>No</i>	<i>Yes</i>	<i>No</i>	<i>No</i>
2	$C/2$	$-D$	<i>Yes</i>	<i>No</i>	<i>No</i>	<i>No</i>
3	$-C/2$	D	<i>No</i>	<i>No</i>	<i>No</i>	<i>Yes</i>
4	$-C/2$	$-D$	<i>No</i>	<i>No</i>	<i>Yes</i>	<i>No</i>

A *Yes* means that both conditions $(x_i + y_i)/2 = a$ and $x_i < y_i$ are true for the corresponding values of C and D , while a *No* is indicated otherwise. Because there is always one and only one *Yes* for each value of i , this table shows the intuitive fact that x and y are uniquely determined from a and b . Besides, if for instance we consider that $(x, y) = (x_2, y_2)$ in Eqs. (13) with $C = 2a$ and $D = \sqrt{12}b$ (corresponding to a *Yes*), we have:

$$x = a - \sqrt{3}b \quad \text{and} \quad y = a + \sqrt{3}b \quad (14)$$

As a direct application of Eqs. (14), it is for instance straightforward to guarantee that $[x, y] \subset [0, 1]$ if, for any $a \in [0, 1]$, b is calculated as

$$\begin{cases} a - \sqrt{3}b \geq 0 \\ a + \sqrt{3}b \leq 1 \end{cases} \Rightarrow b \leq \min \left(a/\sqrt{3}; (1 - a)/\sqrt{3} \right) \quad (15)$$